On periodic homogenization of highly contrasted elastic structures

Lukáš Jakabčin, Pierre Seppecher

On periodic homogenization of highly contrasted elastic structures

Lukáš Jakabčin[1] & Pierre Seppecher[1]

November 25, 2019

Abstract

While homogenization of periodic linear elastic structures is now a well-known procedure when the stiffness of the material varies inside fixed bounds, no homogenization formula is known which enables us to compute the effective properties of highly contrasted structures. Examples have been given in which the effective energy involves the strain-gradient but no general formula provides this strain-gradient dependence. Some formulas have been proposed which involve such terms and provide a small correction to the classical effective energy still when the stiffness of the material varies inside fixed bounds. The goal of this paper is to check the applicability of these formulas for highly contrasted structures. To that aim we focus on structures whose limit energy is already known and we compare the energies given by (i) the convergence results, (ii) the corrective formulas and (iii) by a direct numerical simulation of the complete structure.

Contents

[1]Institut de Mathématiques de Toulon, Université de Toulon, BP 20132, 83957 La Garde Cedex, France. Email: lukas.jakabcin@univ-tln.fr, seppecher@imath.fr.

1 Introduction

Homogenization of periodic elastic materials has been extensively studied. For structures made of different materials with a reasonable contrast, the situation is now well understood and a formula gives the homogenized, or effective, stiffness matrix in terms of the periodically varying one through a cell problem (see for instance [25, 9, 6]). Let us recall this classical result in the 2D case : if $C(y)$ is a Y-periodic stiffness matrix (actually a symmetric bi-linear form on the space of symmetric matrices), then the elastic energy associated to a displacement field $u \in H^1(\Omega, \mathbb{R}^2)$ of the structure contained in a domain Ω reads

$$\mathcal{E}^\varepsilon(u) := \int_\Omega e(u) : \big(C(\frac{x}{\varepsilon}) : e(u)\big)\, dx \tag{1}$$

where $e(u)$ stands for the linearized strain tensor, that is the symmetric part of ∇u, and ε is a small parameter representing the ratio of the "microscopic" periodic length to the "macroscopic" size of Ω. When submitted to a smooth external force field, the equilibrium displacement u^ε minimizes $E^\varepsilon(u) - \int_\Omega f \cdot u$ and thus is solution of the Euler-Lagrange associated equation

$$-\operatorname{div}(C(\frac{x}{\varepsilon}) : e(u)) + f = 0.$$

We say that the structure is "reasonably contrasted" when C belongs to $L^\infty(\Omega)$ and when there exists two positive constants α and β such that, for any matrix M,

$$\alpha\|M\|^2 \leq M : (C : M) \leq \beta\|M\|^2. \tag{2}$$

As ε tends to zero, the sequence u^ε (or a sub-sequence of it) converges to a function u which satisfies the same type of equation where the varying stiffness tensor $C(\frac{x}{\varepsilon})$ is replaced by a constant one C^{hom} : the homogenized (or effective) energy reads

$$\mathcal{E}^{hom}(u) := \int_\Omega e(u) : \big(C^{hom} : e(u)\big)\, dx. \tag{3}$$

The homogenized stiffness matrix can be computed in terms of C by solving, for all symmetric matrices M, the following minimization problem

$$M : \big(C^{hom} : M\big) = \inf_v \int_Y (e(v) + M) : \big(C(y) : (e(v) + M)\big)\, dy \tag{4}$$

This formula, well established from the mathematical point of view, does not apply when the material properties at different points of the structure are so different that their ratio becomes comparable to ε. In that case the tensor $C(y)$ must be replaced by some $C_\varepsilon(y)$ in (1), (2), (4) and the constants α and β in (2) also depend on ε. It is known that, in such highly contrasted structures, the effective behavior can depart from the classical Cauchy elasticity : non-local effects [10, 11, 1] or higher order gradient [24, 14, 1] may appear at the limit. A characterization of all effective behavior which can be achieved has been given in [16].

A great among of work has been devoted to find sufficient conditions in some high contrast cases[1] which forbid such exotic behavior and ensure that formulas (3)-(4) remain valid [23]. We are not here interested in such extensions of the validity domain of the classical formula, but, on the contrary on formulas which give non classical terms in the effective energy. In particular we focus on the case where the homogenized material is a second-gradient or strain-gradient material. This means that the homogenized energy involves the second gradient of the displacement (or equivalently the gradient of the strain field). In addition to C^{hom}, the limit energy represented by a symmetric bi-linear form D^{hom} over right-symmetric third-order tensors and possibly

[1]Note that formulas (3)-(4) may even be valid in the infinite contrast case when holes (part of the material with zero stiffness) are present [23].

a coupling bi-linear form E^{hom} in such a way that the limit energy $\mathcal{E}^{hom}(u)$ reads

$$\int_\Omega \Big(e(u) : \big(C^{hom} : e(u)\big) + \nabla e(u) \vdots \big(D^{hom} \vdots \nabla e(u)\big) + e(u) : \big(E^{hom} \vdots \nabla e(u)\big) \Big)\, dx. \tag{5}$$

There are very few examples of this situation. The first one [24] consists of a material periodically reinforced with parallel, very thin and very stiff cylinders. The second one [14] is the 2D analogous: it consists of a material periodically reinforced with parallel, very thin and very stiff layers. These two examples provide a special case of second gradient materials, called "couple-stress materials" where the second gradient energy involves only the gradient of the skew part of the gradient of the displacement field. A second family of examples was based on the pantograph idea [5, 4, 19, 12, 20, 26]. Indeed a pantograph naturally propagates the deformation. A larger family of examples [1, 2, 3], based on periodic frames, has also been described. For these periodic frames, when the classical homogenization formula gives a degenerate Cauchy material and when one assumes a much stiffer behavior for the material the frame is made of, then one may obtain a second gradient effective material. A process is described in [2] which systematically gives the homogenized energy. This process generally leads to a more complex homogenized behavior where the kinematics needs extra descriptors. The effective behavior is a mix of second-gradient and enriched or generalized continuum. The energy, when expressed in terms of the displacement only, becomes generally non-local.

Up to now there is no criterion to know whether a periodic micro-structure will lead to a second-gradient effective behavior. And, in that case, there is no formula comparable to (3)-(4) for computing higher-order effective stiffness tensors D^{hom} and E^{hom}. Many works have been devoted to the study of corrections at the order ε^2 of formula (3) and second-gradient effects have been obtained in this way (see [27, 7]). The relation between these works and our purpose will be discussed further.

On one hand, a second-gradient model contains intrinsic lengths (any ratio of some coefficient of D^{hom} to some coefficient of C^{hom} is the square of such a length). When the second-gradient effects are corrections at order ε^2, the intrinsic lengths are of order ε. They are then comparable to the size of the periodic cell. There is some paradox in performing homogenization in the desire to ignore variations of displacement at the length-scale of the cells and in obtaining an effective model describing effects at this scale. Moreover such

second-gradient corrections exist when homogenizing diffusion equations as well as when homogenizing elasticity equations while, at the leading order, things are completely different : it has been proved [15, 16] that a second-gradient effective behavior is possible only for elasticity problems. Finally let us remark that corrections can lead to negative higher order stiffness tensor D^{hom} (see [6] for a discussion) while this is clearly impossible at the leading order.

On the other hand, formulas proposed by [27] for computing the corrective terms seem to be very robust. When applied out of their validity domain they still seem to give the right high-order stiffness tensors [21]. The aim of the present paper is to check the robustness of these formulas by considering several situations. For sake of simplicity, let us focus for a while of the non-coupling case when the structure has some symmetry which enforces $E^{hom} = 0$ and let us focus on D^{hom}. In [27], $D^{hom} = \varepsilon^2 \tilde{D}^{hom}$ and a procedure is given for computing $\tilde{D}^{hom}$. This tensor depends on the geometry and on the stiffness of the material at the microscopic level. When the Young modulus is very large, comparable to some negative power of ε, then $\tilde{D}^{hom}$ can become of order ε^{-2} and one recovers a tensor D^{hom} of order one. This is what has been done in [21] where a pantographic-type structure has been considered and second-gradient effects at the leading order have been obtained. The equilibrium state for the resulting macroscopic model has been compared with a direct numerical simulation of the whole detailed structure. Results seem in accordance.

In this paper, in order to further check the formulas given in [27], we apply them to the few cases where the effective behavior has been established. We restrict to 2D cases for sake of simplicity. We first study the case of a layered material, likely the only case where all computations can be performed analytically. Then we study a special case of the frames studied in [1, 2] namely the case of a regular square grid to which we add periodically some diagonals. The effective behavior depends strongly on the way we place these diagonals.

The paper is organized as follows. In Section 3 we recall how the expansion is performed in [27, 8]. We limit the expansion to the second order which is enough for our purpose and avoids many technicalities. We formulate the cell problems which are needed to compute the higher-order terms in the homogenized energy and recall Smyshlyaev-Cherednichenko Theorem. We explain why this theorem should be irrelevant for the examples we will consider.

In Section 4, we nevertheless apply Smyshlyaev-Cherednichenko formulas to the layered case. We get an energy still depending on ε. So we compute its Γ-limit as ε tends to zero. Surprisingly enough, the result coincides with the limit energy stated by Briane and Camar-Eddine [14].

Section 5 is devoted to frame lattices. In section 5.1, we recall the results of Abdoul-Anziz and Seppecher [1]. We apply them to three cases of regular square lattices in which we place diagonals inside the squares in different ways. One case gives a second-gradient effective model, the second one gives a classical Cauchy model while the last one gives a non-local model of Cosserat type. In section 5.2 we compute numerically, for these three cases, the effective high-order stiffness tensors following the procedure of [27] for ε as small as possible. In section 5.3 we study numerically the three global structures with all their details by computing their equilibrium under the effect of a compactly supported external force field. In section 5.4, by a simple optimization method we determine the best macroscopic models (among Cauchy, second-gradient and Cosserat models) which fit the best the global simulation results. In section 5.5, we compare the macroscopic models obtained in the different ways. In the two first cases where respectively a second gradient material and a Cauchy material are expected, the results are concluding. In the last case where a non-local model is predicted by [2] and confirmed by the global simulation, the procedure of [27] gives a second-gradient model whose link to the right macroscopic model is not clear.

2 Notation

In the whole paper we limit ourselves to 2D elasticity problems. We denote (e^1, e^2) the canonical basis of $\mathbb{R}^2$. Following the framework proposed by [27], we define the domain $\Omega = [-T, T]^2$ and we assume that any displacement field u satisfy periodicity boundary conditions: it belongs to the space

$$V := \{u \in H^1(\Omega, \mathbb{R}^2); \int_\Omega u\, dy = 0, u \text{ is } \Omega\text{-periodic}\}.$$

Let $Y = \left[-\frac{1}{2}, \frac{1}{2}\right]^2$. The stiffness fourth-order tensor C is assumed to belongs to $\mathrm{C}^1(\overline{\Omega})$, to be Y periodic and non-degenerate:

$$\exists\ 0 < \alpha < \beta < +\infty,\ \forall M, \quad \alpha\|M\|^2 \leq (C : M) : M \leq \beta\|M\|^2.$$

We are interested in the equilibrium of the linear elastic structure when subjected to an external force field $f \in \mathrm{C}^\infty(\Omega, \mathbb{R}^2)$ satisfying $\int_\Omega f(x)\,dx = 0$. Hence, introducing the linearized strain tensor $e(u)$ associated to the displacement field u by

$$e(u) = \frac{\nabla u + (\nabla u)^t}{2},$$

we are seeking the minimum u_0^ε in V of [2]

$$E_0^\varepsilon(u) := \int_\Omega \Big(\frac{1}{2}\, e(u(x)) : \Big(C\left(\frac{x}{\varepsilon}\right) : e(u(x))\Big) - f(x)\cdot u(x)\Big)\, dx. \tag{6}$$

Following [27], we introduce, for any $\varphi \in Y$ the perturbed problem, consisting in minimizing in V

$$E_\varphi^\varepsilon(u) := \int_\Omega \Big(\frac{1}{2}\, e(u(x)) : \Big(C\left(\frac{x}{\varepsilon} + \varphi\right) : e(u(x))\Big) - f\cdot u(x)\Big)\, dx. \tag{7}$$

Averaging with respect to φ the solution u_φ^ε of this problem leads to the smoothed approximation

$$u^\varepsilon(x) := \int_Y u_\varphi^\varepsilon(x)\, d\varphi. \tag{8}$$

Some results established in this paper use the concept of Γ-convergence [18]. Let us give a simplified definition of Γ convergence valid for our framework.

Definition 2.1 *A sequence of functionals $F_n : L^2(\Omega, \mathbb{R}^2) \to [0, +\infty)$ is said to Γ-converge to the Γ-limit $F : L^2(\Omega, \mathbb{R}^2) \to [0, +\infty)$ if the following two conditions hold for the L^2-strong topology:*

1. *Lower bound inequality: for every sequence $(u_n) \in L^2(\Omega, \mathbb{R}^2)$ converging to u,*

$$F(u) \le \liminf_{n\to+\infty} F_n(u_n)$$

2. *Upper bound inequality: for every $u \in L^2(\Omega, \mathbb{R}^2)$, there is a sequence u_n converging to u such that*

$$F(u) \ge \limsup_{n\to+\infty} F_n(u_n)$$

[2] We use here the double contraction product ":" and $M : (C : M)$ stands for $\sum_{i,j,k,\ell} M_{ij} C_{ijk\ell} M_{k\ell}$.

The reader may refer to [17, 13] for the properties of Γ-convergence. It is important to notice that, provided some compactness properties, Γ-convergence implies convergence of minima, that is of equilibrium solutions.

3 Second-gradient terms appearing in asymptotic expansion

In this section, we describe the formula of Smyshlyaev-Cherednichenko which gives second-gradient terms through an energy expansion.

We need first to introduce the so-called "cell elasticity problem" and its solutions called "correctors":

Definition 3.1 *For any $F \in \mathrm{L}^2(Y, \mathbb{R}^2)$ we define the* cell energy

$$E_F(w) := \int_Y \left(\frac{1}{2}\, e(w) : \Big(C : e(w) \Big) - \Big(F - \int_Y F(z)\, dz \Big) \cdot w \right) dy$$

and we consider the cell elasticity problem

$$(P_F) : \min \left\{ E_F(w);\ w \in H^1(Y),\ \int_Y w\, dy = 0,\ w\ Y\text{-periodic} \right\}.$$

The solution w of this Neumann elasticity problem exists, is unique and satisfies the Euler-Lagrange equation

$$\mathrm{div}(C(y)e(w(y))) + F(y) = \int_Y F(z)\, dz. \tag{9}$$

The first correctors *are the solutions w^{ij} of (P_F) with*[3]

$$F = div_y(C(y)\ : (e^i \otimes e^j)^{sym}). \tag{10}$$

The second correctors *are the solutions z^{ijk} of (P_F) with*

$$F = (C(y)\ : (e^i \otimes e^j)^{sym}) \cdot e^k + (C(y) :\ e_y(w^{ij}(y)) \cdot e^k + div_y(C(y) : \big(w^{ij}(y) \otimes e^k\big)^{sym}\big). \tag{11}$$

[3]The symmetrized tensor product $\otimes$ of two vectors a, $b \in \mathbb{R}^n$ is defined by $(a \otimes b)^{\mathrm{sym}}_{ij} := \frac{a_i b_j + a_j b_i}{2}$.

We are are now in position to define the second-order approximating homogenized energy

Definition 3.2 *We call* second-order energy density *the quadratic form Q^ε which to any second, third and fourth order tensors K, L and M associates*

$$\begin{aligned} Q^\varepsilon(K,L,M) :=& C^{hom}_{(ij)(kl)} K_{ij}(x) K_{kl}(x) + E^{hom}_{(ij)(klm)} K_{ij}(x) L_{klm}(x) \\ &+ D^{hom}_{(ijk)(lmn)} L_{ijk}(x) L_{lmn}(x) + F^{hom}_{(ij)(klmn)} K_{ij}(x) M_{klmn}(x) \\ &+ G^{hom}_{(ijk)(lmnp)} L_{ijk}(x) M_{lmnp}(x) + H^{hom}_{(ijkl)(mnpq)} M_{ijkl}(x) M_{mnpq}(x) \end{aligned}$$

where

$$C^{hom}_{(pr),(kl)} := \int_Y \Big(C : \big(e_y(w^{pr}) + (e^p \otimes e^r)^{sym}\big) \Big) : \big(e_y(w^{kl}) + (e^k \otimes e^l)^{sym}\big)\, dy,$$

$$E^{hom}_{(pr),(klm)} := \varepsilon \int_Y C : (e_y(w^{pr}) + (e^p \otimes e^r)^{sym}) : \big(e_y(z^{klm}) + (w^{kl} \otimes e^m)^{sym}\big)\, dy,$$

$$D^{hom}_{(prs),(klm)} := \varepsilon^2 \left(\int_Y C : (e_y(z^{prs}) + (w^{pr} \otimes e^s)^{sym}) : \big(e_y(z^{klm}) + (w^{kl} \otimes e^m)^{sym}\big)\, dy \right),$$

$$F^{hom}_{(pr),(klmn)} := \varepsilon^2 \left(\int_Y C : (e_y(w^{pr}) + (e^p \otimes e^r)^{sym}) : \big(z^{klm} \otimes e^n\big)^{sym}\, dy \right),$$

$$G^{hom}_{(prs),(klmn)} := \varepsilon^3 \left(\int_Y C : (e_y(z^{prs}) + (w^{pr} \otimes e^s)^{sym}) : \big(z^{klm} \otimes e^n\big)^{sym}\, dy \right),$$

$$H^{hom}_{(prst),(klmn)} := \varepsilon^4 \left(\int_Y C : \big(z^{prs} \otimes e^t\big)^{sym} : \big(z^{klm} \otimes e^n\big)^{sym}\, dy \right).$$

The following theorem states that a fine approximation of the smoothed displacement $u^\varepsilon(x)$ minimizes an energy whose density is Q^ε. We give here a simplified version of [27] restricted to the approximation of order ε^2.

Theorem 3.3 *[Smyshlyaev-Cherednichenko [27]]. Let us define the approximating energy $\mathcal{E}^{SC}_\varepsilon$ by setting, for $v \in V$,*

$$\mathcal{E}^{SC}_\varepsilon(v) := \int_\Omega \Big(\frac{1}{2}\, Q^\varepsilon(e(v), \nabla e(v), \nabla\nabla e(v)) - f \cdot v \Big)\, dx. \tag{12}$$

There exists a constant $\mathcal{K}(f,C,T)$ such that the minimizer v^ε of $\mathcal{E}^{SC}_\varepsilon$ over V satisfies

$$||u^\varepsilon - v^\varepsilon||_{L^2} \le \mathcal{K}(f,C,T)\, \varepsilon^2. \tag{13}$$

The idea of the proof is to construct a fine approximation by defining, for any $v \in C^3(\Omega, \mathbb{R}^2) \cap V$, the expansion

$$u_v(x,\varphi) = v(x) + \varepsilon\, e_{ij}(v(x))\, w^{ij}\left(\frac{x}{\varepsilon} + \varphi\right) + \varepsilon^2\, \partial_k e_{ij}(v(x))\, z^{ijk}\left(\frac{x}{\varepsilon} + \varphi\right),$$

where the functions w^{ij} and z^{ijk} are the correctors introduced in Definition 3.1. Then one computes $E^\varepsilon_\varphi(u_v)$. The mean value of $E^\varepsilon_\varphi(u_v)$ for $\varphi \in Y$ is nothing else than $\mathcal{E}^{SC}_\varepsilon$. The correctors were introduced in such a way that, if v^ε minimises (12), then $div(C : e(u_{v^\varepsilon})) + f$ is of order $O(\varepsilon^2)$. Estimation (13) follows.

The same expansion can still be used for highly contrasted elastic structures that is when the stiffness tensor C is not uniformly bounded with respect to ε, for instance when Y contain two materials A and B with a ratio of shear Lamé coefficients $\dfrac{\mu_B}{\mu_A} = \varepsilon^{-\alpha}$ for some α. All formulas still take sense, but unfortunately, the constant $\mathcal{K}(f, C_\varepsilon, T)$ may become so large that the right-hand side of estimation (13) is no more a small quantity. In that case, the model (12) is no more justified as an approximation of the initial equilibrium solution.

Note that this result is based on an expansion involving the derivative of v up to order two. So the energy density which depends on the first gradient, of this expansion, involve the third derivative of v. This may seem paradoxal as we desire only to take into account the second-gradient terms in the effective energy. The point is that third-gradient terms do provide terms of order ε^2 in $\mathcal{E}^{SC}_\varepsilon$. Note also that terms of order ε^3 and ε^4 are present in $\mathcal{E}^{SC}_\varepsilon$. They ensure the positivity of the quadratic form Q^ε.

As already noticed, Theorem 3.3 does not ensure the accuracy of model (12) for describing the effective behavior of highly contrasted elastic structures. Next sections are devoted to checking the applicability of this model in that case.

4 Material reinforced periodically by stiff layers

Let us describe the first example to which we try to apply the approximation (12). It is the stratified layered material studied by Briane-Camar-Eddine [14]. It is composed periodically with layers made of two different isotropic linear elastic materials A and B.

The rescaled cell $Y = \left[-\frac{1}{2}, \frac{1}{2}\right]^2$ is divided in two parts : δ being a fixed parameter in $(0,1)$, we introduce $Y_B = \left\{ y = (y_1, y_2) \in Y \,/\, |y_2| \leq \frac{\delta}{2} \right\}$ and $Y_A = Y \setminus Y_B$ (see Figure 1). We assume that both parts are made of homogeneous isotropic linear elastic materials which are assumed, for sake of simplicity, to have a vanishing Poisson ratio. Hence the material properties are determined only by the shear modulus $\mu^\varepsilon(y)$ which is assumed to take values $\mu_A = 1$ in Y_A and $\mu_B^\varepsilon = \delta^{-3}\varepsilon^{-2}$ in Y_B.

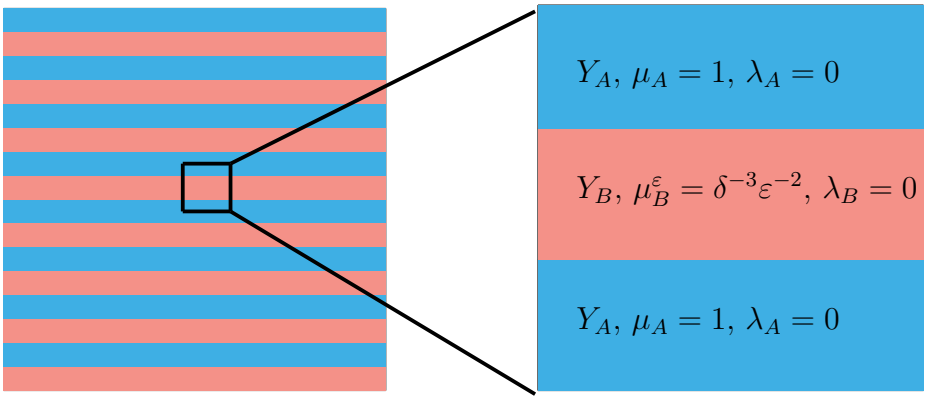

Figure 1: The stratified layered material Ω considered by Briane-Camar-Eddine and the corresponding rescaled cell Y.

The result established in [14] is the following theorem:

Theorem 4.1 *[Briane-Camar-Eddine [14]]. The energy defined over $L^2(\Omega, \mathbb{R}^2)$ by*

$$\mathcal{E}_\varepsilon(v) = \begin{cases} \displaystyle\int_\Omega \mu^\varepsilon \left(\frac{x}{\varepsilon}\right) \|e(u(x))\|^2 \, dx & \text{if } v \in V, \\ +\infty & \text{otherwise.} \end{cases}$$

Γ-converges as ε tens to zero to the functional $\mathcal{E}^{BC}$ defined by

$$\mathcal{E}^{BC}(v) = \int_\Omega \left(\frac{2e_{12}^2(v) + e_{22}^2(v)}{1-\delta} + \frac{1}{12} \left(\frac{\partial^2 v_2}{\partial x_1^2} \right)^2 \right) dx \tag{14}$$

if $v \in V$, $e_{11}(v) = 0$ *a.e. and* $\frac{\partial^2 v_2}{\partial x_1^2}$ *belongs to* $L^2(\Omega)$ *and by* $\mathcal{E}^{BC}(v) = +\infty$ *otherwise.*

In order to apply formula (12) to this case, we now compute the correctors.

4.1 Computation of the first-order correctors

As μ^ε depends only on y_2, $w^{11} = 0$ is clearly the solution of

$$div\Big(2\mu^\varepsilon(y_2)(e_y(w^{11}) + e_1 \otimes e_1)\Big) = 0.$$

Straightforward computations give also the solutions w^{ij} of

$$div\Big(2\mu^\varepsilon(y_2)(e_y(w^{ij}) + \frac{1}{2}(e_i \otimes e_j + e_j \otimes e_i)\Big) = 0.$$

We have $w^{12} = K^\varepsilon r(y_2)\, e^1$ and $w^{22} = K^\varepsilon r(y_2)\, e^2$ where K^ε and r are given by

$$K^\varepsilon := \frac{\mu_B^\varepsilon - \mu_A}{\mu_B^\varepsilon(1-\delta) + \delta\mu_A}, \qquad r(y_2) = \begin{cases} \delta\left(y_2 + \dfrac{1}{2}\right) & \text{if } -\dfrac{1}{2} \le y_2 \le -\dfrac{\delta}{2}, \\ -(1-\delta)y_2 & \text{if } -\dfrac{\delta}{2} \le y_2 \le \dfrac{\delta}{2}, \\ \delta\left(y_2 - \dfrac{1}{2}\right) & \text{if } \dfrac{\delta}{2} \le y_2 \le \dfrac{1}{2}. \end{cases}$$

4.2 Computation of the second-order correctors

We have now to determine six second-order correctors z^{ijk}, solutions of equation (9) with a second member in terms of F given by (11).

The source term in the equation determining z^{111} is written in terms of

$$F = 2\mu^\varepsilon(y_2)(e^1 \otimes e^1)e^1 + 2\mu^\varepsilon(y_2)e_y(w^{11})e^1 + div_y(2\mu^\varepsilon(y_2)(w^{11} \otimes e^1)^{\mathrm{sym}})$$

which reduces to $F = 2\mu^\varepsilon(y_2)e^1$. The partial differential equation for z^{111}, namely,

$$-div_y(2\mu^\varepsilon(y_2)(e_y(z^{111})) = \left(2\mu^\varepsilon(y_2) - \int_Y 2\mu^\varepsilon(y_2)\, dy\right) e^1$$

reduces to an ordinary differential equation whose solution is $z^{111} = g(y_2)e^1$ with $g(y_2) := \left(\dfrac{\mu_A - \mu_B^\varepsilon}{\mu_B^\varepsilon}\right) \tilde{g}(y_2)$ and

$$\tilde{g}(y_2) = \begin{cases} -\delta \left(\dfrac{\mu_B^\varepsilon}{\mu_A}\right) \left(|y_2| - \dfrac{1}{2}\right)^2 + C_1 & \text{if } |y_2| \geq \dfrac{\delta}{2}, \\ (1-\delta)\, y_2^2 + C_2 & \text{if } |y_2| < \dfrac{\delta}{2}. \end{cases}$$

The constants C_1 and C_2 are

$$\begin{aligned} C_1 &= \delta \left(\frac{\mu_B^\varepsilon}{\mu_A}\right) \frac{(1-\delta)^2}{12}(1+2\delta) + \frac{(1-\delta)\delta^3}{6}, \\ C_2 &= -\delta \left(\frac{\mu_B^\varepsilon}{\mu_A}\right) \frac{(1-\delta)^3}{6} + (1-\delta)\delta^2 \frac{(2\delta-3)}{12}. \end{aligned}$$

Similar straightforward but cumbersome computations give $\bar{\bar{w}}^{112} = 0$, $\bar{\bar{w}}^{121} = 0$, $\bar{\bar{w}}^{122} = \bar{\bar{w}}^{221} = K^\varepsilon\, h(y_2)\, e^1$ and $\bar{\bar{w}}^{222} = K^\varepsilon\, h(y_2)\, e^2$ where h is the function defined by

$$h(y_2) = \begin{cases} -\dfrac{\delta}{2} \left(|y_2| - \dfrac{1}{2}\right)^2 + \dfrac{1-\delta^2}{12} & \text{if } |y_2| \geq \dfrac{\delta}{2}, \\ \dfrac{1-\delta}{2} \left(y_2^2 + \dfrac{\delta(\delta-2)}{12}\right) & \text{if } |y_2| < \dfrac{\delta}{2}, \end{cases}$$

4.3 Determination of the second-order elastic energy

Determining explicitly all the tensors in Definition 3.2, is again a straightforward but tedious computation. We obtain[4]

$$\begin{aligned}\mathcal{E}_\varepsilon^{SC}(v) = \frac{1}{2}\int_\Omega \Bigg[& M^\varepsilon (e_{11})^2 + 4H^\varepsilon (e_{12})^2 + 2H^\varepsilon (e_{22})^2 + \theta^\varepsilon \left(e_{11,1}\right)^2 + \gamma^\varepsilon \left(e_{12,1}\right)^2 \\ & + \int_Y \mu^\varepsilon(y) \left(e_{11} + \varepsilon^2 \left(g(y) e_{11,1,1} + K^\varepsilon h(y)(2e_{12,2,1} + e_{22,1,1})\right)\right)^2 dy \\ & + \varepsilon^4 \int_Y \mu^\varepsilon(y) \left(g(y) e_{11,1,1} + K^\varepsilon h(y) \left(2e_{12,2,1} + e_{22,1,1}\right)\right)^2 dy \\ & + \varepsilon^4 \int_Y \mu^\varepsilon(y) \left(g(y) e_{11,1,2} + K^\varepsilon h(y) \left(e_{22,2,1} + 2e_{12,2,2} + e_{22,1,2}\right)\right)^2 dy \\ & + \varepsilon^4 \int_Y 2\mu^\varepsilon(y) (K^\varepsilon h(y))^2 \left(e_{22,2,2}\right)^2 dy \Bigg] dx.\end{aligned}$$

where

$$\begin{aligned} M^\varepsilon &:= \int_Y \mu^\varepsilon(y)\, dy = \mu_A(1-\delta) + \delta\mu_B^\varepsilon, \\ H^\varepsilon &:= \left(\int_Y \frac{1}{\mu^\varepsilon(y)}\, dy\right)^{-1} = \frac{\mu_A \mu_B^\varepsilon}{\mu_B^\varepsilon(1-\delta) + \delta\mu_A}, \\ \theta^\varepsilon &:= \frac{2}{3}\frac{\varepsilon^2(\mu_B^\varepsilon - \mu_A)^2(1-\delta)^2\delta^2}{H^\varepsilon}, \\ \gamma^\varepsilon &:= \frac{2}{3}\frac{\varepsilon^2 M^\varepsilon (1-\delta)^2\delta^2(\mu_B^\varepsilon - \mu_A)^2}{(\mu_B^\varepsilon(1-\delta) + \delta\mu_A)^2}. \end{aligned}$$

For further purpose, let us notice that, when ε tends to zero, the constants entering this expression have the following behavior:

$$M^\varepsilon \sim \delta\mu_B^\varepsilon, \quad H^\varepsilon \sim \frac{\mu_A}{1-\delta}, \quad \theta^\varepsilon \sim \frac{2}{3}\frac{\varepsilon^2(\mu_B^\varepsilon)^2\delta^2(1-\delta)^3}{\mu_A}, \quad \gamma^\varepsilon \sim \frac{2}{3}\varepsilon^2\mu_B^\varepsilon\delta^3.$$

4.4 Limit as ε goes to zero

In this section we prove that the Smyshlyaev-Cherednichenko approximation that we just recalled, converges for the L^2-strong topology to the model (14)

[4]Here, for lightening the expression, we have simply denoted e_{ij} the quantity $e_{ij}(v)$ and $e_{ij,k}$ or $e_{ij,k,\ell}$ the quantities $\frac{\partial e_{ij}(v)}{\partial x_k}$ or $\frac{\partial^2 e_{ij}(v)}{\partial x_k \partial x_\ell}$. In a similar way $v_{i,j,k}$ stands for $\frac{\partial^2 v_i}{\partial x_j \partial x_k}$.

obtained by Briane and Camar-Eddine [14].

Theorem 4.2 *The energy $\mathcal{E}_\varepsilon^{SC}$ Γ-converges, as $\varepsilon \to 0$, to $\mathcal{E}^{BC}$.*

Proof Here C is a positive constant which may vary from line to line. Let $(v^\varepsilon) \subset V$ be a sequence such that $\mathcal{E}_\varepsilon^{SC}(v^\varepsilon) < C < \infty$. As the energy contains only positive terms, we have

$$M^\varepsilon (e_{11}(v^\varepsilon))^2 \leq C, \quad H^\varepsilon (e_{12}(v^\varepsilon))^2 \leq C, \quad H^\varepsilon (e_{22}(v^\varepsilon))^2 \leq C.$$

As M^ε tends to infinity and H^ε tends to $1/(1-\delta)$, we deduce that $e(v^\varepsilon)$ is bounded in L^2 and, by Korn inequality, that v^ε is bounded in H^1: there exists some $v \in H^1$ such that, up to a sub-sequence, v^ε converges to v strongly in L^2. Moreover $e_{11}(v) = 0$. We have

$$\mathcal{E}_\varepsilon^{SC}(v^\varepsilon) \geq \frac{1}{2} \int_\Omega \left(4H^\varepsilon (e_{12}(v^\varepsilon))^2 + 2H^\varepsilon (e_{22}(v^\varepsilon))^2 + \gamma^\varepsilon (e_{12,1}(v^\varepsilon))^2 \right) dx$$

and, as γ^ε tends to $2/3$, we obtain

$$\liminf_{\varepsilon \longrightarrow 0} \mathcal{E}_\varepsilon^{SC}(v^\varepsilon) \quad \geq \quad \frac{1}{2} \int_\Omega \left(\frac{4(e_{12}(v))^2 + 2(e_{22}(v))^2}{1-\delta} + \frac{2}{3}(e_{12,1}(v))^2 \right) dx.$$

under the constraint $e_{11}(v) = 0$. This constraint allows us to rewrite $e_{12,1}(v) = \frac{1}{2}(v_{2,1,1} + v_{1,2,1}) = \frac{1}{2} v_{2,1,1}$. The right-hand side of the last estimation thus coincides with $\mathcal{E}^{BC}(v)$.

In order to prove the $\Gamma - \limsup$ inequality, we consider by density $v \in C^\infty(\overline{\Omega}, \mathbb{R}^2)$ such that $e_{11}(v) = 0$. We simply set $v^\varepsilon = v$ and we have

$$\begin{aligned} \limsup_{\varepsilon \to 0} \left(\mathcal{E}_\varepsilon^{SC}(v^\varepsilon) \right) = \lim(H^\varepsilon) \times \int_\Omega \left((2(e_{12}(v))^2 + (e_{22}(v))^2) \right) dx \\ + \lim \left(\frac{\gamma^\varepsilon}{2} \right) \times \int_\Omega \left(e_{12,1}(v) \right)^2 dx + \frac{1}{2} \lim \Big(\int_Y \mu(y) \varepsilon^4 \left(K^\varepsilon h(y) \right)^2 dy \Big) \times \\ \int_\Omega \left(2e_{22,2,2}^2 + (e_{22,2,1} + 2e_{12,2,2} + e_{22,1,2})^2 + 2(2e_{12,2,1} + e_{22,1,1})^2 \right) dx. \end{aligned}$$

As $\int_Y \mu(y) \varepsilon^4 \left(K^\varepsilon h(y) \right)^2 dy$ tends to zero, we finally get

$$\limsup_{\varepsilon \to 0} \left(\mathcal{E}_\varepsilon^{SC}(v^\varepsilon) \right) = \mathcal{E}^{BC}(v).$$

□

5 Lattices

In the following subsections we restrict our attention to a soft material reinforced by a very stiff regular square grid Ω containing diagonals distributed in different ways. We consider successively grids that are characterized by the following periods:

- Case 1: a square grid with one row over two reinforced by diagonals (see Figure 2),
- Case 2: a pure square grid (see Figure 3),
- Case 3: a square grid reinforced by one diagonal every four squares (see Figure 4).

We choose as unit length the global size L of Ω: $L = 1$. Each structure contains $2n + 1$ vertical bars and we define $\varepsilon = 1/n$. All bars have the same thickness $\eta = \varepsilon^2$. A choice of the force unit allows us to fix the shear modulus of material under the form

$$\mu^\varepsilon = \frac{1}{2}\varepsilon^{-3}. \tag{15}$$

For sake of simplicity we fix to zero the second Lamé coefficient $\lambda^\varepsilon = 0$. This assumption is not essential and the results are similar when dealing with a non-vanishing Poisson ratio.

In the sequel we study each of the three considered structures using three different methods.

First we compute the Γ-limit as ε tends to zero of the elastic energy using the results of [1, 2]. The three considered cases have been chosen in such a way that their limit energies are of different types. For using the results of [1, 2] we must assume that the weak part of the structure is made by voids. Using these results when the shear modulus of the weak part of the structure is non zero but of order ε needs a technical extension of the theorem of [1] which would be out of place in this paper.

Secondly, we apply the results of [27] for different values of n, i.e. of ε, by computing numerically the first and second correctors. This needs, on the contrary, that the weak part of the structures is not void. We thus obtain in each case a macroscopic description taking into account the possibility of second-gradient effects.

In a third time we perform, for different values of ε, a numerical simulation of the whole elastic structure by computing its equilibrium state under the

action of a particular external force field. We search among different models, which one describes the best this equilibrium state.

Finally we compare the results given by the three methods.

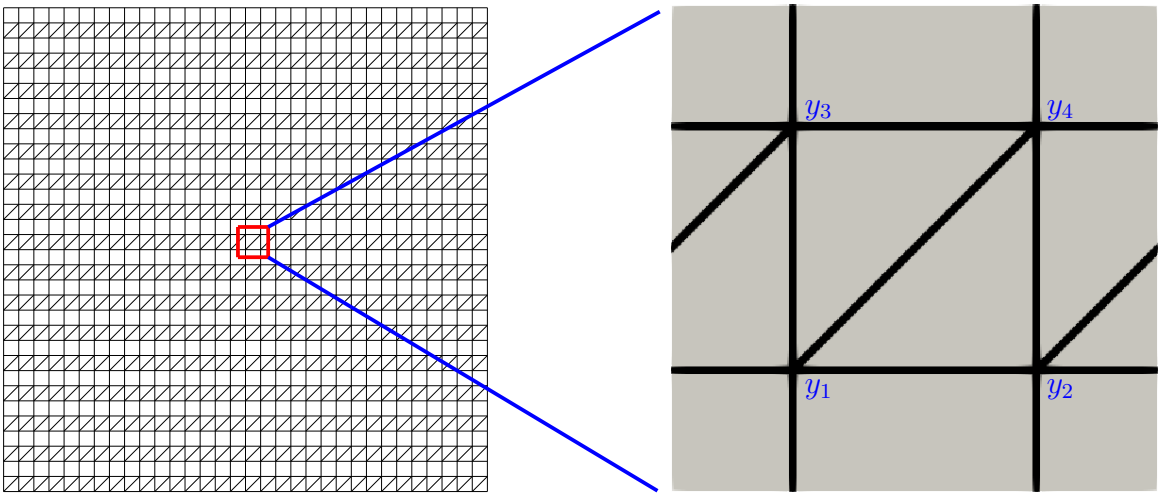

Figure 2: A square grid - case 1 (left) with its cell (right)

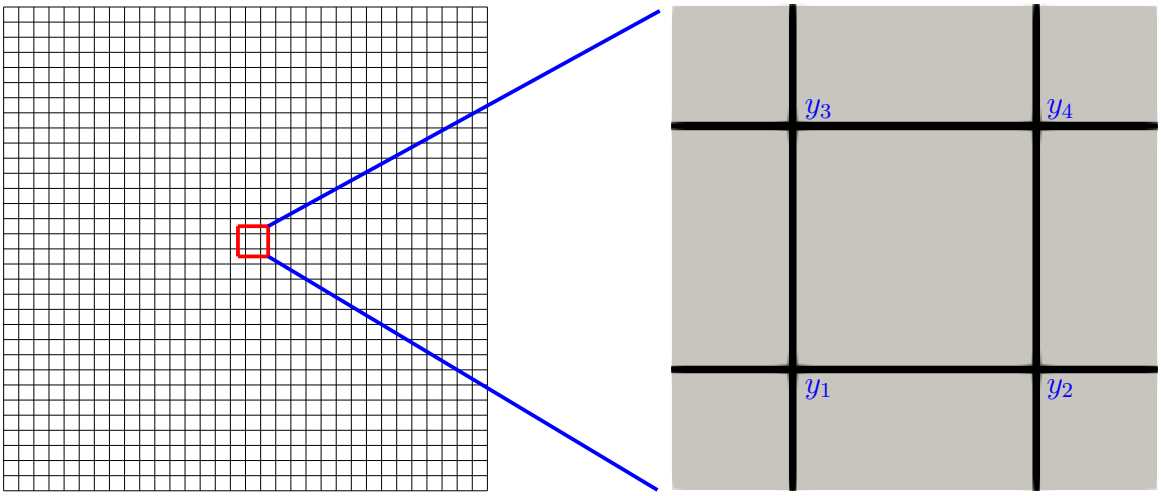

Figure 3: A square grid - case 2 (left) with its cell (right)

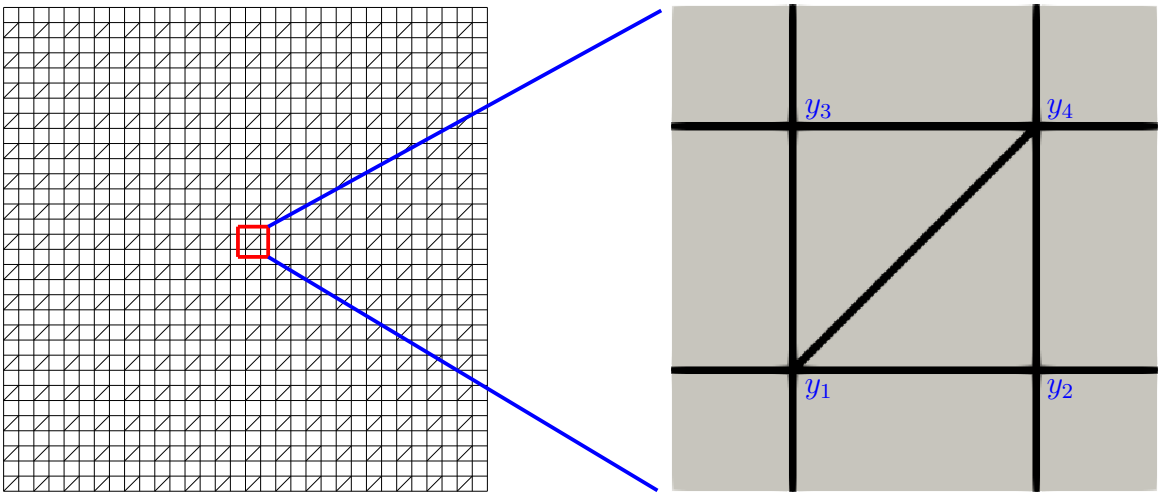

Figure 4: A square grid - case 3 (left) with its cell (right)

5.1 Abdoul-Anziz-Seppecher high contrast homogenization

In [1, 2, 3] is provided a general method for obtaining the limit behavior of periodic graph-based elastic structures. For using this method we must first describe, according to [1], the periodic structures we consider in this section: in the orthonormal basis (e^1, e^2), the rescaled cell Y is the square $[0,1]^2$; it contains four nodes $y_1 = 0$, $y_2 = e^1/2$, $y_3 = e^2/2$, $y_4 = e^1/2 + e^2/2$; the small parameter ε (assumed to be the inverse of some integer) characterizes the small periodicity vectors which are here εe^1 and εe^2, thus the nodes of the structures are the points $y_{i,j,s} = \varepsilon(y_s + ie^1 + je^2)$ for all $s \in \{1,2,3,4\}$ and $(i,j) \in \{1,\dots,1/\varepsilon\}^2$. The three considered cases differ only by the way the nodes are linked by elastic bars. As the sub-structures linking the nodes are very thin, it has been proved in [1] that they act like Euler-Bernouilli beams : the limit energy is also the limit energy of a discrete system of nodes where only global extensional stiffness (spring-like stiffness) and global bending stiffness of these beams play a role. Each node $y_{i,j,s}$ is endowed with a mean displacement $U_{i,j,s}$ and rotation $\theta_{i,j,s}$ and the discrete energy is the

sum

$$\sum_{(i,j,r,s)} \frac{a_{1,r,s}}{2}\Big(\rho^{0,0}_{i,j,r,s}+\varepsilon^2\alpha^{0,0}_{i,j,r,s}\Big)+\frac{a_{2,r,s}}{2}\Big(\rho^{1,0}_{i,j,r,s}+\varepsilon^2\alpha^{1,0}_{i,j,r,s}\Big) + \frac{a_{3,r,s}}{2}\Big(\rho^{0,1}_{i,j,r,s}+\varepsilon^2\alpha^{0,1}_{i,j,r,s}\Big) \qquad (16)$$

where the quantities

$$\rho^{k,\ell}_{i,j,r,s} := \Big(\frac{U_{i+k,j+\ell,s}-U_{i,j,r}}{\varepsilon}\cdot\tau^{k,\ell}_{r,s}\Big)^2$$

$$\alpha^{k,\ell}_{i,j,r,s} := \left(\frac{\theta_{i+k,j+\ell,s}+\theta_{i,j,r}}{2}-\frac{U_{i+k,j+\ell,s}-U_{i,j,r}}{\varepsilon\ell^{k,\ell}_{r,s}}\cdot\big(\tau^{k,\ell}_{r,s}\big)^{\perp}\right)^2+\left(\frac{\theta_{i+k,j+\ell,s}-\theta_{i,j,r}}{12}\right)^2$$

stand for the global extension and bending deformations of the bar which links nodes $y_{i+k,j+\ell,s}$ and node $y_{i,j,r}$. Here we have set $\ell^{k,\ell}_{r,s} := \|y_r - y_s + ke^1 + \ell e^2\|$ and $\tau^{k,\ell}_{r,s} := (y_r - y_s + ke^1 + \ell e^2)/\ell^{k,\ell}_{r,s}$. The ratio ε^2 between extensional and bending energies in (16) is due to the fact that all bars of the structures have the same thickness ε^2. The extensional stiffness can be computed by taking into account the length, the thickness of the bars as well as the Lamé coefficients (15) of the material they are made of: we have $a_{1,r,s} = 1/\ell^{0,0}_{r,s}$, $a_{2,r,s} = 1/\ell^{1,0}_{r,s}$ and $a_{3,r,s} = 1/\ell^{0,1}_{r,s}$. Of course, we set $a_{p,r,s} = 0$ whenever the nodes are not directly linked. In the three cases the matrices[5] a_p take the form

$$a_1=\begin{pmatrix}0&2&2&\xi\\0&0&0&2\\0&0&0&2\\0&0&0&0\end{pmatrix},\ a_2=\begin{pmatrix}0&0&0&0\\2&0&\zeta&0\\0&0&0&0\\0&0&2&0\end{pmatrix},\ a_3=\begin{pmatrix}0&0&0&0\\0&0&0&0\\2&0&0&0\\0&2&0&0\end{pmatrix}$$

where $(\xi,\zeta)=(\sqrt{2},\sqrt{2})$ in case 1, $(\xi,\zeta)=(0,0)$ in case 2, $(\xi,\zeta)=(\sqrt{2},0)$ in case 3.

The results of [1] give an algebraic procedure which allows us to compute the limit behavior of the structures as ε tends to zero. In this limit, the effective material becomes inextensible in the horizontal and vertical directions: $e_{11}(u) = e_{22}(u) = 0$. Only the shear $e_{12}(u)$ remains free and the energy becomes:

[5]Note that the matrices a_4 and a_5 evoked in [1] vanish in our cases.

- Case 1: $\dfrac{1}{2}\displaystyle\int_\Omega \left(50.3\Big(e_{12}(u)\Big)^2 + \frac{1}{2}\left(\frac{\partial e_{12}(u)}{\partial x_1}\right)^2\right) dx$
- Case 2: $\dfrac{1}{2}\displaystyle\int_\Omega 16\Big(e_{12}(u)\Big)^2 dx$
- Case 3:

$$\inf_\Phi \frac{1}{2}\int_\Omega \left(32\Big(e_{12}(u)\Big)^2 + \frac{1}{4}\|\nabla\Phi\|^2 + 17.04\left(\frac{1}{2}\left(\frac{\partial u_2}{\partial x_1} - \frac{\partial u_1}{\partial x_2}\right) - \Phi\right)^2\right) dx$$

These limit energies correspond respectively to a second-gradient model, a standard Cauchy model and a non-local Cosserat-type model. The two first cases have already been studied in [1, 2] where the qualitative behavior of the limit energies were described. At our knowledge the third case is new. It provides one of the simplest examples of convergence of a sequence of classical elasticity energies toward a Cosserat-type model.

5.2 Smyshlyaev-Cherednichenko approximation

Now we compute the Smyshlyaev-Cherednichenko approximation for fixed values of ε. In each case, we have to solve successively i) (9) with source (10) which gives the first correctors w^{ij}; ii) compute the new source (11); iii) solve again (9) with this new source and finally iv) compute the numerous tensors involved in Definition 3.2.

The problems we have to solve are classical Neumann elasticity problems set in the rescaled periodic cell $Y = [0,1] \times [0,1]$ with periodic boundary conditions. The cell is made by two parts: a stiff one Y_ε where $\mu^\varepsilon = 0.5\,\varepsilon^{-3}$ and a weak one $Y \setminus Y_\varepsilon$ where $\mu^\varepsilon = 0.5\,\varepsilon$. The stiff part is still the union of very thin rectangles whose thickness is now ε. Hence we need to use an extremely thin mesh in order to describe the fields inside Y_ε in an accurate way: the mesh size Δx is chosen such that ε is approximately $5\Delta x$ (see Figure 5). The variational formulation of the cell elasticity problems are solved by a finite elements method using FreeFem++©[22].

We have studied different values of ε ($\varepsilon = 1/40$ or $\varepsilon = 1/60$). The value $n = 1/\varepsilon = 60$ corresponds to the maximal number of cells that we will be able to study in next section where the whole structure is simulated.

We first notice that C^{hom}_{1111} and C^{hom}_{2222} are extremely large which corresponds to the expected inextensibility in the horizontal and vertical directions ($e_{11}(u) = e_{22}(u) \sim 0$). Hence we focus on terms relative to $e_{12}(u)$: we define

$$c^{SC} := C_{(12)(12)};$$
$$a^{SC} := \varepsilon^2 D_{(121)(121)} - \varepsilon^2 E_{(12)(1211)}.$$

which we call respectively "shear and bending coefficients".

These coefficients are summarized in Tables 1, 2 and 3.

n	ε	c^{SC}	a^{SC}
40	0.025	0.122	14
60	0.017	0.124	14.51

Table 1: Shear and bending coefficients in Case 1

n	ε	c^{SC}	a^{SC}
40	0.025	0.0004	4.33
60	0.017	0.0002	4.39

Table 2: Shear and bending coefficients in Case 2

n	ε	c^{SC}	a^{SC}
40	0.025	0.0306	8.84
60	0.017	0.031	9.15

Table 3: Shear and bending coefficients in Case 3

We have also checked that the small value of μ^ε in the weak part of the cell was irrelevant by choosing different values (keeping the same order of magnitude): shear and bending are insensitive to these changes. This justifies our comparison of the results obtained in this subsection with the results obtained in the previous and next subsections where μ^ε is assumed to vanish in the weak part.

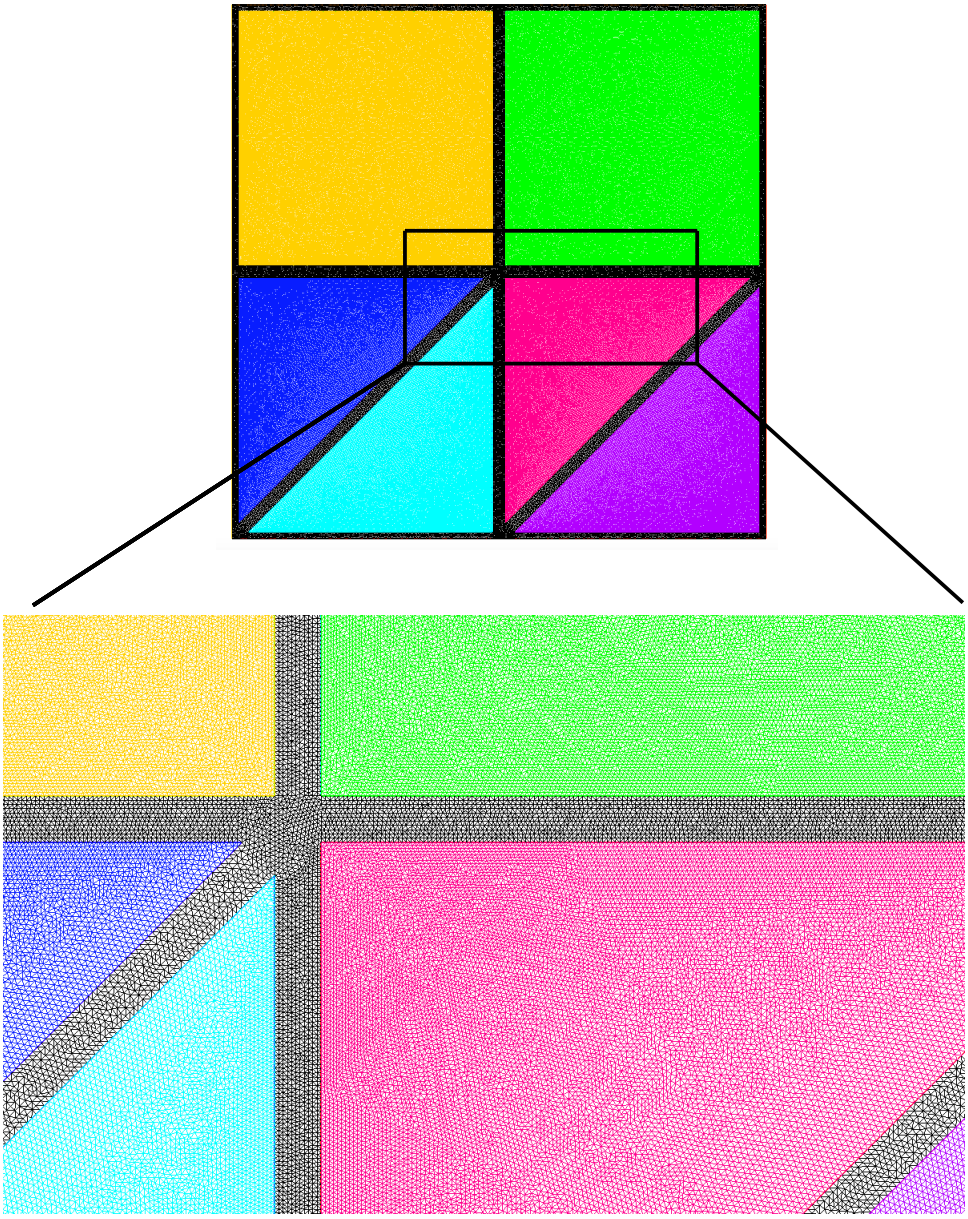

Figure 5: Meshing the rescaled cell Y for Case 1.

5.3 Global numerical simulation

Now we study the global behavior of the three structures made by $n \times n$ cells (see Figures 2 3 4). We assume Dirichlet boundary conditions on the lateral sides of Ω and periodicity conditions on the top and bottom sides. Then we subject the structures to a balanced system of forces F. We choose the force field for obtaining an equilibrium displacement essentially vertical and ε-periodic in the vertical direction: we set $F(x_1, x_2) := (0, f(x_1))$ with

$$f(x_1) = \begin{cases} 1 & \text{if } |x_1| \leq 1/8, \\ -1 & \text{if } 1/8 < |x_1| \leq 1/4, \\ 0 & \text{if } |x_1| > 1/4. \end{cases}$$

Due to computational cost, we avoid meshing the weak part of the structure by assuming, like in Section 3, that the weak part is void. This forbids the presence of forces applied in the void part. So we replace f by an approximation f_ε obtained by concentrating f on the vertical stiff bars. The independence of such vertical forces with respect to x_2 associated to the periodic boundary conditions in x_2 ensures that the equilibrium displacement field is ε periodic with respect to x_2. Hence we can reduce our study to the domain $[-1/2, 1/2] \times [0, \varepsilon]$: we denote Ω_ε the part of this domain where the material lies (see Figure 6).

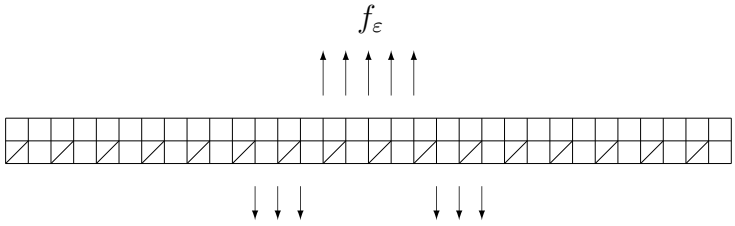

Figure 6: Ω_ε and the applied forces f_ε

We solve numerically the elasticity problem

$$\min_u \int_{\Omega_\varepsilon} \left(\frac{1}{2} \left(C \left(\frac{x}{\varepsilon} \right) e(u(x)) \right) \cdot e(u(x)) - F \cdot u(x) \right) dx$$

where the displacement field u is periodic on top and bottom side of Ω_ε and satisfies a Dirichlet boundary condition on left and right side. The numerical implementation realized with FreeFem++© by finite elements method,

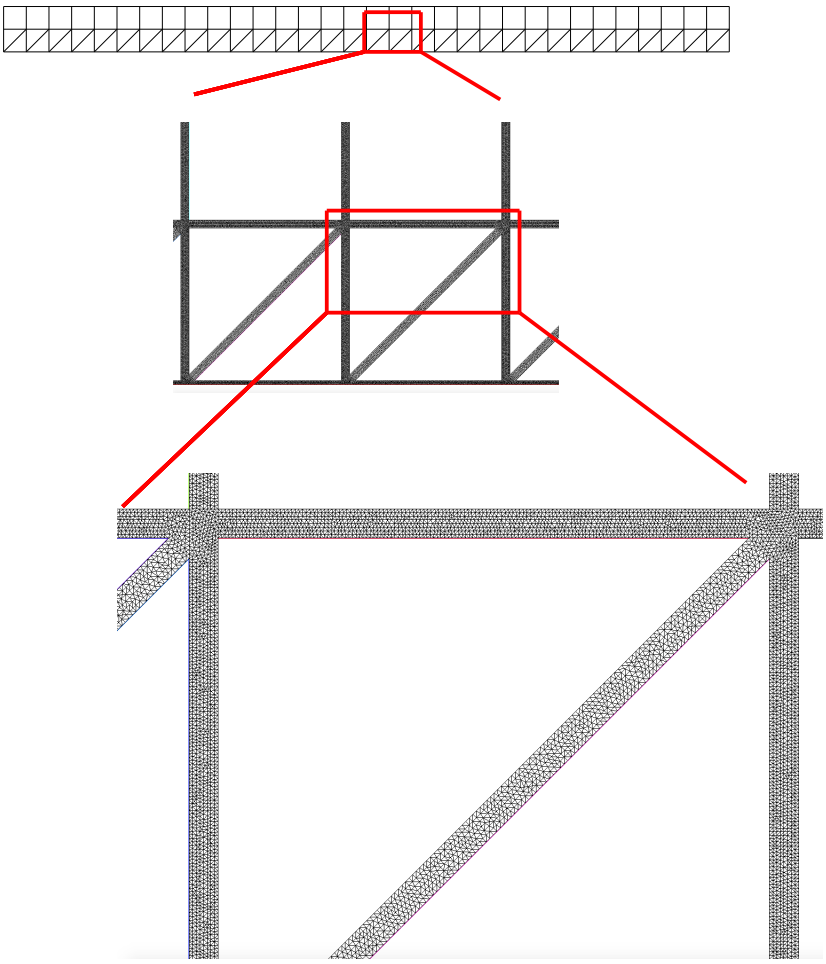

Figure 7: Zoom on the mesh

needs approximately 700 000 P1-elements (see Figure 7). As expected, the displacement field converges as $\varepsilon \to 0$ or equivalently as $n \to +\infty$. For instance, we plotted in Figure 8a the vertical displacement (measured on the horizontal middle line of the domain) corresponding to Case 3. As expected oscillations at the length scale ε of the cells and with amplitude of order ε are observed. Convergence is clearer in Figure 8b where we used a moving average (using a trick similar to (8)).

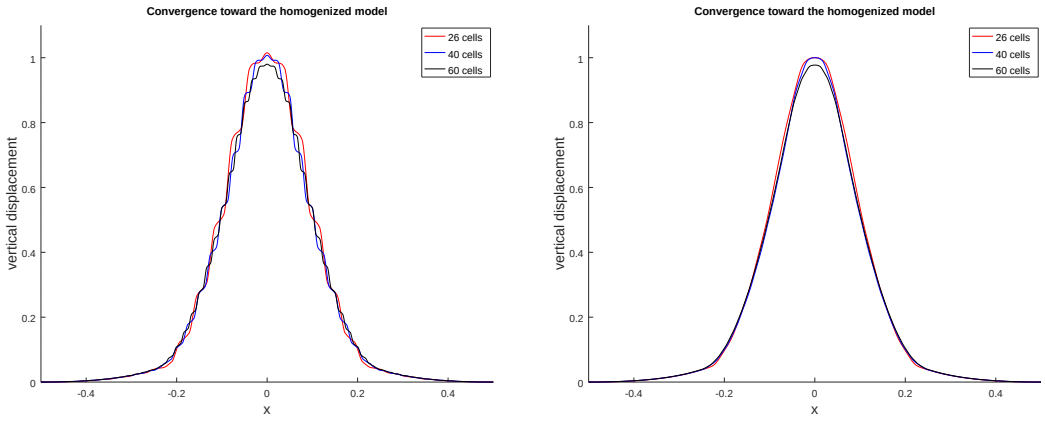

Figure 8: The vertical displacement for the Case 3 with $n = 26, 40, 60$ cells.

In the sequel we present only the results obtained for $n = 60$.

5.4 Fitting a macro-model for global simulation results

The numerical simulations performed in the previous section provide a vertical displacement field u^{NS} as a function of x_1. Now we search which macroscopic model provides a similar displacement. We search this model among the family of mixed second-gradient and Cosserat-type models, that is models whose elastic energy, in terms of the displacement field, takes the form

$$E(u) = \inf_{\Phi} \frac{1}{2} \int_\Omega \Big((\mathbb{A} : (\Phi - (\nabla u)^{skew})) : (\Phi - (\nabla u)^{skew}) + (\mathbb{B} \vdots \nabla\Phi) \vdots \nabla\Phi + (\mathbb{C} : e(u)) : e(u) + (\mathbb{D} \vdots \nabla e(u)) \vdots \nabla e(u) \Big) \, dx$$

where $(\nabla u)^{skew} := \frac{\nabla u - (\nabla u)^t}{2}$ stands for the skew-symmetric part of ∇u. Indeed all the models which have been obtained in [14, 27, 1, 2] enter this class

of models. The periodicity of the structure implies that the effective model is homogeneous (the tensors $\mathbb{A}$, $\mathbb{B}$, $\mathbb{C}$ and $\mathbb{D}$ of respective orders 4, 6, 4 and 6 must be constant). The assumptions made on the external force field and on the boundary conditions (note that we assume the same boundary conditions for ϕ as we did for u) ensure that the equilibrium solution is a vertical displacement $(0, u_2)$ depending only on the horizontal variable x_1 and that Φ has the form $\Phi = \begin{pmatrix} 0 & -\phi(x_1) \\ \phi(x_1) & 0 \end{pmatrix}$. Hence $\nabla u = \begin{pmatrix} 0 & 0 \\ u_2'(x_1) & 0 \end{pmatrix}$ and the equilibrium problem reduces to a one-dimensional variational problem :

$$\min_{(u_2,\phi)} \int_{-1/2}^{1/2} \Big(a\,(\phi - \frac{1}{2}u_2^{'})^2 + b\,(\phi^{'})^2 + c\,(u_2^{'})^2 + d\,(u_2^{''})^2 - 2f(x_1)\,u_2 \Big)\, dx_1. \quad (17)$$

where $a := 8\mathbb{A}_{1212}$, $b := 4\mathbb{B}_{121121}$, $c := 4\mathbb{B}_{1212}$, $d := 4\mathbb{D}_{121121}$. The minimization is performed under the boundary conditions $u_2(-1/2) = u_2(1/2) = 0$, $\phi(-1/2) = \phi(1/2) = 0$. It can be performed analytically but it is more convenient to compute the solution of problem (17) by solving under Octave© the linear problem associated to the 1D Euler - Lagrange equation discretized by the finite difference method.

For each quadruplet (a, b, c, d), we compute the solution $(u, \phi)_{a,b,c,d}$ of problem (17) and we compute the relative error

$$\Delta_{(a,b,c,d)} := \frac{||u_{(a,b,c,d)} - u^{NS}||_{L^2}}{||u^{NS}||_{L^2}}$$

to the solution u^{NS} provided by the global numerical simulation. Finally, using a simplex method with Octave© we determine the optimal (a^*, b^*, c^*, d^*) which minimizes $\Delta_{(a,b,c,d)}$.

- **Case 1:** Square grid with rows of diagonals. We obtain the following optimal parameters:

n	a	b	c	d	$\Delta_{(a,b,c,d)}$
60	0	0	15.7	0.124	0.51%

  The model we obtain in this way is clearly a second-gradient model as $a = b = 0$. The relative error is very small. Indeed the equilibrium displacement obtained with this model fits well with the displacement obtained through the global simulation (see Fig. 9). One could wonder

if a classical Cauchy models could also fit the curve obtained through the global simulation. To check that point, we also searched the best Cauchy model by seeking among parameters of type $(0, 0, c, 0)$ which one fits the best the numerical curve. The relative error is much larger as it can be seen in Fig. 9.

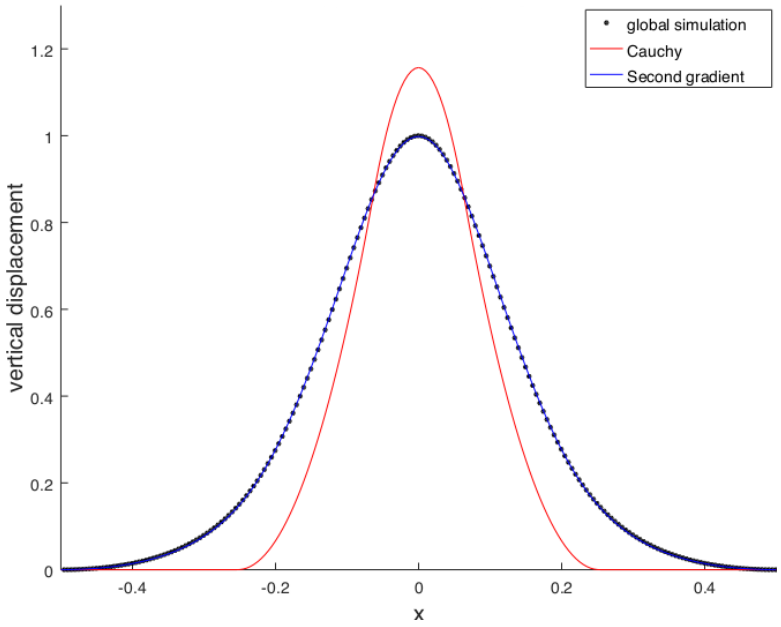

Figure 9: The best second-gradient and Cauchy models for describing the global simulation of the vertical displacement of the structure in Case 1.

- **Case 2:** Reinforcement by a square grid. In that case we get

n	a	b	c	d	$\Delta_{(a,b,c,d)}$
60	0	0	4.64	0	1.54%

  The model corresponds now clearly to a classical Cauchy material. It still fits well with the displacement field obtained through global simulation (see Fig. 10).

- **Case 3:** Reinforcement by a square grid with isolated diagonals. Results obtained in that case are presented in the following table.

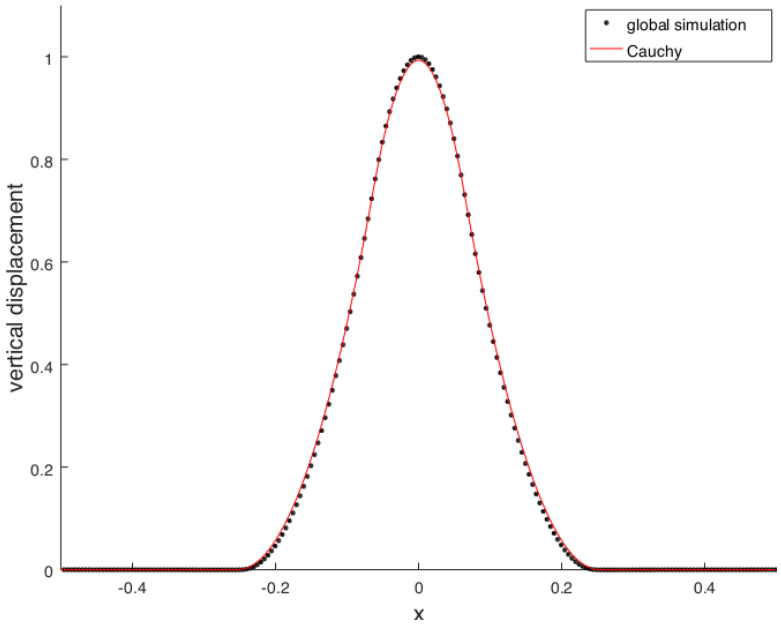

Figure 10: The best Cauchy approximation to the global simulation of the displacement in Case 2.

n	a	b	c	d	$\Delta_{(a,b,c,d)}$
60	15.9	0.192	9.24	0	0.47%

The optimal set of parameters gives again a model which fits extremely well the displacement field obtained through the global simulation (see Fig. 11). It corresponds to a Cosserat-type material. In order to check whether a classical Cauchy model or a second gradient model would also be able to fit the numerical curve we performed also the optimization among the sets of parameters of type $(0, 0, c, 0)$ or $(0, 0, c, d)$. The curves corresponding to these partially optimal sets of parameters are shown in Fig. 11: The Cauchy model is clearly out of order; the second-gradient model is better but the relative error is 5.47% that is tenth times larger than for the Cosserat model. One can remark, in particular, that the second-gradient model is not able to accurately describe the deformation of the structure in its free part (i.e. when $|x_1| > 1/4$).

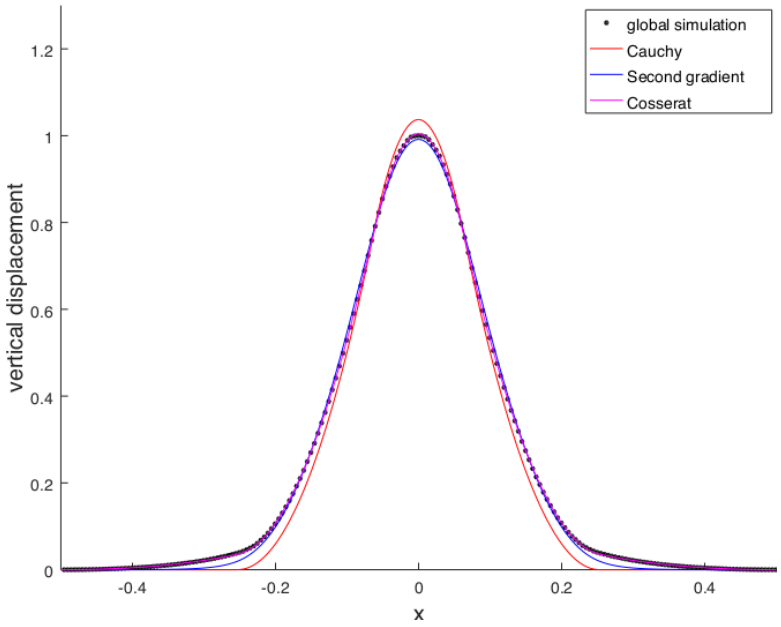

Figure 11: The best Cosserat, second gradient and Cauchy models approximation to the global simulation in Case 3.

5.5 Comparison and interpretation of the results

We resume in Table 4 the set of parameters (a, b, c, d) which have been obtained through the three different approaches: (i) the best set for fitting the global simulation, (ii) the parameters predicted by Smyshlyaev and Cherednichenko, (iii) the parameters predicted by Abdoul-Anziz and Seppecher.

Note first that Anziz-Seppecher approach is relative to the limit model as ε tends to zero while the other approaches focus on structures where ε is small but fixed. This explains the slight discrepancy between the values obtained in this way and the global simulation. Note also that Smyshlyaev-Cherednichenko approach gives, when the contrast is assumed to be not too high, an approximation of the equilibrium displacement field with an error of order ε^2. This also explains a slight discrepancy. This being said, for Case 1 and Case 2 in which the effective models are second gradient and Cauchy models, results coincide in a reasonable way. In Case 3, where the effective model is a Cosserat one as predicted by Anziz-Seppecher approach and confirmed by the global simulation, Smyshlyaev-Cherednichenko approach

Case 1	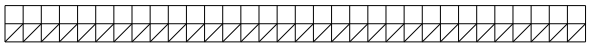			
	a	b	c	d
Global simulation	0	0	15.7	0.124
Smysh.-Cherednich.	0	0	14.51	0.124
Anziz-Seppecher	0	0	12.	0.125
Case 2	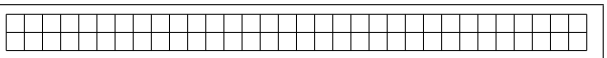			
	a	b	c	d
Global simulation	0	0	4.64	0
Smysh.-Cherednich.	0	0	4.39	0.0002
Anziz-Seppecher	0	0	4	0
Case 3	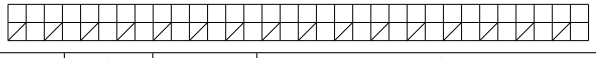			
	a	b	c	d
Global simulation	15.9	0.19	9.24	0
Smysh.-Cherednich.	0	0	9.15	0.031
Anziz-Seppecher	17.0	0.25	8	0

Table 4: Material parameters determined by the different approaches

provides instead a second-gradient model.

6 Conclusion

In a rather surprising way the formula proposed in [27] and suggested by an asymptotic expansion gives, even when applied completely out of its scope, excellent results in all known cases of second-gradient effective behavior. We conjecture that, provided that we know a priori that the effective energy is of second-gradient type, the limits as ε tends to zero of formulas (12) give the effective tensors. However, from the practical point of view, this conjecture does not seem very useful. Indeed, in view of the examples described in Sections 5.3 and 5.4, we do not see emerging any criterion for a priori know the type of the effective energy. It remains an open question to identify such a criterion and to prove (or contradict) the aforementioned conjecture.

Acknowledgement

The authors acknowledge the support of the French *Agence Nationale de la Recherche* (ANR), under grant ANR-17-CE08-0039 (project ArchiMatHOS).

References

[1] Houssam Abdoul-Anziz and Pierre Seppecher. Homogenization of periodic graph-based elastic structures. *Journal de l'Ecole polytechnique–Mathmatiques*, 5:259–288, 2018.

[2] Houssam Abdoul-Anziz and Pierre Seppecher. Strain gradient and generalized continua obtained by homogenizing frame lattices. *Mathematics and Mechanics of Complex Systems*, 6(3):213–250, 2018.

[3] Houssam Abdoul-Anziz, Pierre Seppecher, and Cédric Bellis. Homogenization of frame lattices leading to second gradient models coupling classical strain and strain-gradient terms. *Mathematics and Mechanics of Solids*, 24(12):3976–3999, 2019.

[4] Jean-Jacques Alibert and A Della Corte. Second-gradient continua as homogenized limit of pantographic microstructured plates: a rigorous proof. *Z. Angew. Math. Phys.*, 66(5):2855–2870, 2015.

[5] Jean-Jacques Alibert, Pierre Seppecher, and Francesco dell'Isola. Truss modular beams with deformation energy depending on higher displacement gradients. *Mathematics and Mechanics of Solids*, 8(1):51–73, 2003.

[6] Grégoire Allaire. Homogenization and two-scale convergence. *SIAM Journal on Mathematical Analysis*, 23(6):1482–1518, 1992.

[7] Grégoire Allaire, Marc Briane, and Muthusamy Vanninathan. A comparison between two-scale asymptotic expansions and bloch wave expansions for the homogenization of periodic structures. *SeMA Journal*, 73(3):237–259, 2016.

[8] Nikolai Sergeevich Bakhvalov and G Panasenko. *Homogenisation: averaging processes in periodic media: mathematical problems in the mechanics of composite materials*, volume 36. Springer Science & Business Media, 2012.

[9] A. Bensoussan, J-L. Lions, and G. Papanicolau. *Asymptotic Analysis for Periodic Structures*. North-Holland, Amsterdam, 1978.

[10] G. Bouchitté and Bellieud M. Homogenization of elliptic problems in a fiber reinforced structure. non local effects. *Ann. Scuola Norm. Sup. Cl. Sci.*, IV(26):407?436, 1998.

[11] G. Bouchitté and Bellieud M. Homogenization of a soft elastic material reinforced by fibers. *Asymptotic Analysis*, (32):153–183, 2002.

[12] C. Boutin, F. dell'Isola, I. Giorgio, and L. Placidi. Linear pantographic sheets: Asymptotic micro-macro models identification. *MEMOCS*, 5(2):127–162, 2017.

[13] Andrea Braides. Γ-*convergence for Beginners*. Oxford University Press, 2002.

[14] Marc Briane and Mohamed Camar-Eddine. Homogenization of two-dimensional elasticity problems with very stiff coefficients. *Journal de mathmatiques pures et appliques*, 88(6):483–505, 2007.

[15] M Camar-Eddine and P Seppecher. Closure of the set of diffusion functionals with respect to the Mosco-convergence. *Mathematical Models and Methods in Applied Sciences*, 12(08):1153–1176, 2002.

[16] Mohamed Camar-Eddine and Pierre Seppecher. Determination of the closure of the set of elasticity functionals. *Archive for Rational Mechanics and Analysis*, 170(3):211–245, 2003.

[17] Gianni Dal Maso. *An Introduction to* Γ*-Convergence*. Birkhuser, Boston, 1993.

[18] E De Giorgi. Sulla convergenza di alcune successioni dintegrali del tipo dellarea. *Ennio De Giorgi*, 414, 1975.

[19] F dell'Isola, I Giorgio, Marek Pawlikowski, and N.L. Rizzi. Large deformations of planar extensible beams and pantographic lattices: Heuristic homogenization, experimental and numerical examples of equilibrium. *Proceedings of the Royal Society. Series A: Mathematical, Physical and Engineering Sciences*, 472(2185), 2016.

[20] F DellIsola, I Giorgio, Marek Pawlikowski, and NL Rizzi. Large deformations of planar extensible beams and pantographic lattices: Heuristic homogenization, experimental and numerical examples of equilibrium. *Proceeding of the Royal Society of London, Sries A: Mathematical, Physical and Engineering sciences*, 472(2185), 2016.

[21] Baptiste Durand, Arthur Lebee, and Sab Karam. Numerical study of pantographs. Personal communication, 2019.

[22] Frédéric Hecht. New development in freefem++. *Journal of numerical mathematics*, 20(3-4):251–266, 2012.

[23] O. A. Oleinik, A.S. Shamaev, and G. A. Yosifian. *Mathematical problems in elasticity and homogenization*. North-Holland, Amsterdam, 1992.

[24] Catherine Pideri and Pierre Seppecher. A second gradient material resulting from the homogenization of an heterogeneous linear elastic medium. *Continuum Mechanics and Thermodynamics*, 9(5):241–257, 1997.

[25] Enrique Sanchez-Palencia. *Non homogeneous media and vibration theory*. Springer-Verlag, Berlin, 1980.

[26] Pierre Seppecher, Jean-Jacques Alibert, and Francesco dellIsola. Linear elastic trusses leading to continua with exotic mechanical interactions. *Journal of Physics: Conference Series*, 319(1), 2011.

[27] V. P. Smyshlyaev and K. D. Cherednichenko. On rigorous derivation of strain gradient effects in the overall behaviour of periodic heterogeneous media. *Journal of the Mechanics and Physics of Solids*, 48:1325–1357, 2000.